scientific reports

Check for updates

OPEN

Chemical composition of antimicrobially active fractions derived from extract of filamentous fungus *Keratinophyton Lemmensii* including three novel bioactive compounds

Roman Labuda[1,2]✉, Markus Bacher[2,3], Thomas Rosenau[3,6], Hannes Gratzl[2,4], Maria Doppler[2,4], Sonja Hager[5], Doris Marko[5], Christoph Wiesner[8], Monika Očková[8], Nicole Ollinger[9], Martin Wagner[1], Christoph Schüller[2,7] & Joseph Strauss[2,7]✉

Screening for new bioactive microbial metabolites, we found a novel okaramine derivative, for which we propose the trivial name lemmokaramine, as well as two already known okaramine congeners – okaramine H and okaramine J - responsible for antimicrobial activity of the recently described microscopic filamentous fungus, *Keratinophyton lemmensii* BiMM-F76 (= CCF 6359). In addition, two novel substances, a new cyclohexyl denominated lemmensihexol and a new tetrahydroxypyrane denominated lemmensipyrane, were purified and characterized. The compounds were isolated from the culture extract of the fungus grown on modified yeast extract sucrose medium by means of flash chromatography followed by preparative HPLC. The chemical structures were elucidated by NMR and LC-MS. The new okaramine (lemmokaramine) exerted antimicrobial activity against Gram-positive and Gram-negative bacteria, yeasts and fungi and anticancer activity against different mammalian cell lines (Caco-2, HCT116, HT29, SW480, MCM G1, and MCM DLN). Furthermore, we found a significant antioxidant effect of lemmokaramine following H_2O_2 treatment indicated by activation of the Nrf2 pathway. This is the first report describing analysis and structural elucidation of bioactive metabolites for the onygenalean genus *Keratinophyton*.

Keywords Fungal metabolites, Keratinophilic fungi, Okaramines

The microscopic fungus, *Keratinophyton lemmensii* (*Ascomycota*, *Onygenales*, *Onygenaceae*), has been isolated during a mycological survey of a compost sample from an agriculture base at the Institute of Agrobiotechnology

[1]Unit of Food Microbiology, Department for Farm Animals and Veterinary Public Health, Institute of Food Safety, Food Technology and Veterinary Public Health, University of Veterinary Medicine Vienna, Veterinaerplatz 1, 1210 Vienna, Austria. [2]Core Facility Bioactive Molecules, Screening and Analysis and Research Platform Bioactive Microbial Metabolites (BiMM), Konrad Lorenz Strasse 24, 3430 Tulln an der Donau, Austria. [3]Institute of Chemistry of Renewable Resources, Department of Chemistry, University of Natural Resources and Life Sciences, Vienna (BOKU), Konrad Lorenz Strasse 24, 3430 Tulln an der Donau, Austria. [4]Department of Agrobiotechnology (IFA-Tulln), Institute of Bioanalytics and Agro-Metabolomics, University of Natural Resources and Life Sciences, Vienna (BOKU), Konrad Lorenz Strasse 20, 3430 Tulln an der Donau, Austria. [5]Department for Food Chemistry and Toxicology, Faculty of Chemistry, University of Vienna, Waehringerstrasse 38, 1090 Vienna, Austria. [6]Johan Gadolin Process Chemistry Centre, Åbo Akademi University, Porthansgatan 3, 20500 Turku, Finland. [7]Department of Applied Genetics and Cell Biology, Institute of Microbial Genetics, University of Natural Resources and Life Sciences, Vienna (BOKU), Konrad Lorenz Strasse 24, 3430 Tulln an der Donau, Austria. [8]Department of Medical and Pharmaceutical Biotechnology, IMC University of Applied Sciences Krems AT, 3500 Krems, Austria. [9]FFoQSI – Austrian Competence Centre for Feed and Food Quality, Safety & Innovation, Stelzhamerstr. 23, 4600 Wels, Austria. ✉email: roman.labuda@vetmeduni.ac.at; joseph.strauss@boku.ac.at

(IFA- Tulln), Austria and described as a novel taxon[1]. In general, the genus *Keratinophyton* is represented by a large group of keratinolytic soil-born fungi rather common especially in areas with high animal activity that results in transfer of the keratinous material, such as fur, hairs, hoofs, etc. to the soil. Ecology and distribution of the genus has been reviewed in a previous study by Labuda et al. (2021, 2024). Currently, this genus comprises a total of 29 recognized and accepted taxa[2,3]. Fungi are able to produce a tremendous number of substances called secondary metabolites. Among the secondary metabolites are substances involved in processes affecting fungal biology[4], the biosphere[5], and also frequently in human medical issues[6]. Synthesis of such secondary metabolites is organized and regulated in biosynthetic gene clusters (BCGs)[4]. Fungi from the order Onygenales seem to have a large biosynthetic potential with pathways that are specific to Onygenales fungi and have not been found elsewhere[7]. Among other unique characteristics, *K. lemmensii* differs from its relatives by production of a bright yellow pigment on some media (e.g., on potato dextrose agar), and inhibition of several microorganisms in vitro. This bioactivity sparked our interest since there has been no previous report dealing with the chemistry of metabolites produced by the genus *Keratinophyton* or related *Aphanoascus*. In addition the genus likely represents a generally unexplored source of possible new bioactive compounds[8]. Therefore, the goal of this study was to investigate presence and structural elucidation of secondary metabolites responsible for the bioactivity of the fungus, *K. lemmensii*.

Here we report compound isolation, bioactivity tests, and structure elucidation of a new okaramine congener denominated lemmokaramine, a novel cyclohexyl derivative lemmensihexol and a novel tetrahydroxypyrane named lemmensipyrane.

Materials and methods

Fungal isolation and taxonomy

Detailed information about origin of the microscopic filamentous fungus *Keratinophyton lemmensii* BiMM-F76 collected 2015 in a sample of a compost at base of IFA Tull (Austria) has been reported earlier[1]. Molecular markers (DNA sequences) of the fungus are deposited in GenBank for MN633082 (ITS), and MT874998 (LSU).

A simple screening method to test antimicrobial activity in vitro (agar-plug method)

An agar plug, i.e., colony and agar under the colony, were taken off by the cork borer (9 mm in diam.) from a culture of *Keratinophyton lemmensii* BiMM-F76, growing on Yeast Extract Agar (YES) plate for 14 days at 25 °C, in dark. The plug was then applied on a plate in upright position (by agar side down), with a spread tester microorganism and cultivated at 37 °C, overnight (8–16 h), in darkness. The tester microorganism was spread ~ 30 min before the plug is applied to allow physiological solution to diffuse into a medium. Here *Staphylococcus aureus* ATCC 6538 (SA), *Pseudomonas aeruginosa* ATCC 9027 (PA), *Klebsiella pneumoniae* ATCC 10,031 (KL), *Escherichia coli* ATCC 25,922 (EC), *Candida albicans* ATCC 10,231 (CA), and *Aspergillus fumigatus* RL 578 (AFu), were used as indicator microorganisms. The positive reaction is visible as an active zone around the agar plug (inhibition halo) and might be expressed in mm diam. This method has been adopted according to the simple screening method for detection of intracellular and extracellular secondary metabolites produced by filamentous fungi for the thin layer chromatography[9].

Fermentation and extraction

The fungal spore suspension (5.0×10^6 spores/mL) was obtained after 7 days cultivation of the fungus (*K. lemmensii* BiMM-F76) on a potato dextrose agar (PDA, Van Waters and Rogers (VWR) International, Leuven, Belgium, Austria). Five colony plugs were cut (each ca. 1 × 1 cm) and thoroughly mixed (on vortex for 2 min) with 30 mL of physiological solution (0.9% NaCl) in a sterile, 50 mL Falcon tube. In total, 4 L of yeast extract sucrose agar medium (YES, Samson et al., 2000) spread over approximately 160 Petri dishes, was used for production of secondary metabolites. The production medium (YES) was modified by reduction of the total content of sucrose (from 15 to 5%) and agar-agar (from 2 to 0.5%). Each plate was inoculated with 100 µL of spore suspension in three parallel streaks at the central and subcentral part of the plate. The plates were cultivated in perforated plastic bags for seven weeks at 25 °C, in the dark. At the end of the cultivation, the plates were checked for purity, cut into small pieces and the whole content of the plates (fungal colonies with medium) was harvested into a 5 L glass flask. The material was then mixed with 4 L of ethyl acetate. After vigorous stirring for 2 min in three subsequent steps (with ca. 20 min in between), the mixture was filtered through a steel sieve in order to separate the solid particles (fungus and medium). The remaining residual water (generated by condensation of the water on plates during fungal growth) was removed by the addition of ~ 30 g of anhydrous sodium sulphate. The organic phase was then filtered through a filter paper (270 mm i.d., Macherey-Nagel, Düren, Germany) and concentrated under reduced pressure at 45 °C (Büchi Rotavapor R-114, Flawil, Switzerland). The whole extraction procedure was repeated three times and yielded ~ 4 g of crude oily culture extract. The crude extract in the study has been designated under a number #197 (indicating a batch number, further necessary also for tracing the down-stream process in isolation and elucidations). The aliquot of the crude extract was tested against the pathogens (SA, PA, KL, EC, CA, Afu) by disc diffusion method, where 40 µL containing 250–300 µg of the extract was applied on Whatman filter paper disc and after solvent evaporated (at 45 °C, for 30 min.) it was applied directly on plate with spread pathogen and cultivated at 37 °C, overnight (8–16 h), in darkness. The crude extract showed activity against *Staphylococcus aureus* (SA) and *Candida albicans* (CA), with ~ 25 mm inhibition zones around discs. These positive reactions of the extract led to further isolation of active principles described below.

Isolation of secondary metabolites

The crude extract was purified as previously described (Labuda et al., 2021) by reversed-phase silica gel vacuum flash chromatography (Interchim, puriFlash®450, Montlucon CEDEX, France), using three consecutive

Interchim puriFlash® 32 g silica IR-50C18-F0025 flash columns (particle size: 50 µm). The columns were eluted with a binary solvent gradient (solvent A: H2O, solvent B: ACN). The starting linear gradient from 10% B to 27% B during 25 min at a flow rate 15 mL/min was followed by an isocratic gradient at 52% B for 10 min. Then a linear gradient from 52 to 66% B over 7 min was applied at the same flow rate and finally the column was washed starting with 100% B for 10 min followed by 100% A for 10 min at a flow rate 15–30 mL/min. UV 254 nm and UV scan 200–400 nm modes were used for detection and final separation of 6 main fractions (F1–F6), which were used for activity test and consequently concentrated under reduced pressure at 45 °C. Whole pre-purification (flash chromatography, Figure S32) was repeated four times (one gram of the crude extract per run-chromatography cycle). An aliquot (40 µL) from each fraction was tested for its target antimicrobial activity (against SA and CA) by the disc diffusion method as described above. The target activity against SA and CA was spotted in fraction F4 (21–35 min Rt, yield: 550 mg) and F5 (35–47 min Rt, yield: 880 mg). Consequently, the two active fractions were resolved in a solvent mix (1:1:1; ACN/CH3OH/H2O) and further individually purified by an Agilent 1260 Infinity preparative HPLC (Agilent, Santa Clara, CA, USA) on a reversed phase column Gemini NX C-18 (21.20×150 mm, 5 µm, 110 Å). Gradient starting with 30% ACN and 70% H2O up to 90% ACN in 10 min (total time 34 min) and a flow rate of 25 mL/min.

Five subfractions of fraction F4 (i.e., F4pF1–pF5, time slice each 1 min) were collected after the first step preparation, of which pF4 (12–15 min Rt) and pF5 (15–20 min Rt) contained the active targets (both subfractions showed activity against SA and CA). As the both active subfractions contain the mixture of several substances, the second preparative step was necessary and resulted in isolation of active substances, cyclo (6a′-(α,α-dimethylallyl)-$_L$-Trp-$_L$-Trp) (**5**) (as substance F4pF4.4, 16.5 min Rt, yield: 4.5 mg), and cyclo (N^8-(α,α-dimethylallyl)-$_L$-Trp-$_L$-Trp) (**4**) (as substance F4pF5.3, 28.5 min Rt, yield: 1.5 mg). Four subfractions of fraction F5 (i.e. F5pF1–pF4, time slice 1 min) were collected after first step preparation, tested against the target microorganisms (as above) and resulted in identification of two active fractions, representing **a novel substance** similar to okaramine H, = lemmokaramine (**1**) (as substance F5pF3-4, 22.5 min Rt, yield: 23 mg). The additional two inactive sub-fractions were found to be represented by cyclo (N^8-(α,α-dimethylallyl)-$_L$-Trp-6a′-(α,α-dimethylallyl)-$_L$-Trp) (**6**) (as substance F5pF1, 23.5 min Rt, yield: 7.7 mg), and okaramine H (**2**) (as substance F5pF2, 23 min Rt, yield: 8.9 mg). Apart of foregoing okaramine congener (**2**) and related compounds (**4**, **5**, **6**), two novel compounds, namely a novel tetrahydropyrane = lemmensipyrane (**7**) (as substance F4pF2.2, 19.8 min Rt, yield: 11.3 mg), and novel cyclohexyl = lemmensihexol (**10**) (as substance F4pF3.2, 18 min Rt, yield: 17.6 mg) were isolated and identified in inactive fractions F4pF2 and F4pF3, respectively. For purity check (Figure S8), an Agilent 1200 system was used with the same stationary phase (Gemini 5 µm NX-C18 110 Å, 150×2 mm) and gradient pro-gram at a flow rate 0.3 mL/min.

LC-MS and NMR

A diluted solution of the purified metabolite was measured with liquid chromatography-high resolution mass spectrometry. Chromatographic separation was carried out with a reverse phase C18 column (Gemini ®, NX-C18, 5 µm, 110 Å, 150×2 mm, Phenom-enex, Torrance, CA, USA) in an UHPLC-system (Vanquish-Thermo Fisher Scientific, Bre-men, Germany). 5 µL of sample solution were injected and gradient elution was carried out using H_2O and MeOH each containing 0.1% formic acid (FA) as eluent A and B respectively. The flow rate was set to 0.3 mL/min and the column was kept at 25 °C. After two minutes of linear elution with 50% B, a 30 min gradient to 45% B followed by three minutes constant 95% B and re-equilibration of the system with 50% B for ten minutes was applied resulting in a chromatographic method of 60 min. The UHPLC-system was coupled to a QExactive HF Orbitrap mass spectrometer (Thermo Fisher Scientific, Bremen, Germany) via a heated ESI interface operating in fast-polarity switching mode (positive/negative ionization). Full MS and MS/MS scan events using an inclusion list were carried out for the positive and negative ionization mode. Full scan mass spectra were recorded in profile mode with a scan range m/z 100–1000 and a resolution of 120,000 FWHM (at m/z 200). If ions listed in the inclusion list were present in the full scan mass spectra, MS/MS was triggered with an isolation window of m/z ± 1 and collision energy (25 eV) in the HCD collision cell. MS/MS fragment spectra were recorded with a resolution setting of 15,000 FWHM (at m/z 200). Manual data evaluation was carried out with Thermo Scientific™ Xcalibur™ software.

All NMR spectra were recorded on a Bruker Avance II 400 (Rheinstetten, Germany) (resonance frequencies 400.13 MHz for ^{1}H and 100.63 MHz for ^{13}C) equipped with a 5 mm N_2-cooled cryo probe head (Prodigy) with z-gradients at room temperature with standard Bruker pulse programs. The sample was dissolved in 0.6 mL of MeOD (99.8% D) and a few drops of DMSO-d6 (99.8% D). Chemical shifts are given in ppm, referenced to residual solvent signals (3.31 ppm for ^{1}H, 49.0 ppm for ^{13}C). ^{1}H NMR data were collected with 32k complex data points and apodized with a Gaussian window function (lb = −0.3 Hz and gb = 0.3 Hz) prior to Fourier transformation. ^{13}C spectrum with WALTZ16 ^{1}H decoupling was acquired using 64k data points. Signal-to-noise enhancement was achieved by multi-plication of the FID with an exponential window function (lb = 1 Hz). All two-dimensional experiments were performed with 1k × 256 data points, while the number of transients (2–16 scans) and the sweep widths were optimized individually. HSQC experiment was acquired using adiabatic pulse for inversion of ^{13}C and GARP-sequence for broadband ^{13}C-decoupling, optimized for ^{1}J(CH) = 145 Hz. For the NOESY spectrum a mixing time of 0.8 s was used.

Antimicrobial activity

Minimal inhibitory concentrations (MIC) were quantified according to EUCAST guidelines (http://www.eucast.org, accessed on: 20. 10. 2020). The following microorganisms were used: bacteria: *Staphylococcus aureus* ATCC 6538 (Gram-positive), *Escherichia coli* ATCC 25,922, *Klebsiella pneumoniae* ATCC 10,031 and *Pseudomonas aeruginosa* ATCC 9027 (Gram-negative); yeast fungus *Candida albicans* ATCC 10,231, and the filamentous

fungus *Aspergillus fumigatus* (RL578). Concentration range of the compound tested for the evaluation of the antimicrobial activity was 0,5–650 µg/mL.

Cytotoxicity assay

For cytotoxicity tests cells were seeded in 96 well plates at a density of 5×10^5 (CaCo-2) or 2×10^5 (melanoma) cells per well and incubated 24 h. The potential cytotoxic effect was determined by using a resazurin-based in vitro toxicology assay (Sigma-Aldrich; Schnelldorf, Germany), according to the instructions of the manufacturer with slight modifications[11]. Briefly, cells were grown to 90% confluence and treated for 24 h with lemmokaramine (**1**) diluted in fresh media at 37 °C. Subsequently, cells were washed and incubated with 10% resazurin in fresh medium for 1.5 h. In a microplate reader with fluorescence mode (544 nm excitation, 590 nm emission; POLARstar Omega, BMG LABTECH, Ortenberg, Germany), the reduced form of resazurin (resorufin) was quantified. Data were analyzed using OmegaMARS Data analysis software package (BMG LABTECH, Ortenberg, Germany). Cell viability was normalized to untreated cells grown under the same conditions. Lemmokaramin (**1**) was measured on two days each in triplicate ($n=3$). For cytotoxicity tests with HCT116, SW480 and HT29 cells, cells were seeded (2×10^3 cells/well or 3×10^3 cells/well for HT29) in 96-well plates. After 24 h recovery, cells were treated with **1** for 72 h. For analysis, cells were incubated with a 1:10 dilution of CellTiter-Blue (CTB, Promega) solution in the respective cell medium for 1 h at 37 °C and 5% CO_2. Fluorescent signals of supernatants were measured utilizing a Synergy H1 hybrid multimode reader (BioTek, Bad Friedrichshall, Germany) at 560 nm_{ex}/590 nm_{em}.

Cell culture

Human Caco-2 cells were purchased from DSMZ (Braunschweig, Germany), and maintained in MEM with Earle's salts and non-essential amino acids supplemented with 10% FBS and 100 µg mL − 1 penicillin/streptomycin (P/S). Human colon carcinoma HCT116, SW480 and HT29 cells were purchased from American Type Culture Collection (Manassas, USA) and maintained in DMEM GlutaMAX supplemented with 10% FBS and 1% P/S, MEM supplemented with 10% FBS, 1% P/S and 1% L-glutamin or in DMEM with 10% FBS and 1% P/S, respectively. Cells were grown at 37 °C in a humidified atmosphere (≥95%) with 5% CO2. Preliminary tests showed that up to 1% DMSO concentration had no impact on viability of cells. The used concentration was 0.8%. MCM 1G and MCM DLN (kindly provided by P. Petzelbauer, Department of Dermatology, Medical University of Vienna, Austria) were cultured in MIM media and at 37 °C in a humidified atmosphere containing 5% CO_2[11]. Briefly, the MIM medium was prepared by mixing 14.08 g of MCDB 153 medium (M7403, Sigma-Aldrich) in 800 mL ddH_2O, followed by the addition of 12.6 mL sodium bicarbonate (7.5%) (S8761; Sigma-Aldrich), adjusting the pH to 7.4, and sterile filtration. In addition, 200 mL of L-15 (Leibovitz) medium (L1518; Sigma-Aldrich), 20 mL FCS (10270-106; ThermoFisher Scientific, Waltham, MA, USA), 10 mL penicillin/streptomycin (15140-122; ThermoFisher Scientific), 0. 5 mL insulin (I9278, Sigma-Aldrich), 1680 µL calcium chloride solution (21115, Sigma-Aldrich), 2 µg/mL ciprofloxacin (17850-5G-F, Sigma-Aldrich), and 50 ng/mL EGF (53003-018, ThermoFisher Scientific) were added. Cells were passaged every 3–5 days until 80% confluence was reached.

Decatenation assay

To detect the catalytic activity of topoisomerase II α, a decatenation assay using catenated kinetoplast DNA (kDNA) was performed. The total reaction volume was fixed to 20 µL. In brief, assay buffer (50 µM Tris-HCl; pH 8; 150 mM NaCl; 10 mM $MgCl_2$; 2 mM ATP and 0.5 mM DTT) containing kDNA (200 ng) (TopoGen Inc., Buena Vista, CO, USA) and the tested drugs were added to 0.8 U of human topoisomerase II α. After 1 h of incubation at 37 °C, the reaction was ended by adding the stop buffer (TopoGEN Inc.; 1% Sarkosyl, 0.025% bromphenolblue, 5% glycerol). Doxorubicin (10 µM) was used as a positive control. The reaction mixtures were run on a 1% w/v agarose gels with Tris-acetate/EDTA (TAE) buffer at 4.5 V/cm. The gel was stained in 10 mg/L of ethidium bromide solution for 20 min. Fluorescence signals were detected with Image Quant LAS-4000 (GE Healthcare Life Sciences, Buckinghamshire, UK). Fujifilm Image Gauge software (Fujifilm Medical Systems USA, Inc., Lexington, MA USA) was used to detect decatenated DNA.

Gyrase inhibition assay

To detect the catalytic activity of gyrase, a supercoiling assay using relaxed DNA (rel. DNA) was performed. The total reaction volume was fixed to 20 µL. In brief, assay buffer (7 mM Tris-HCl; pH 7.5; 4.8 mM KCl; 0.8 mM $MgCl_2$; 0.2 mM ATP, 1.3% glycerol, 0.36 mM spermidine, 20 µg/ml BSA and 0.4 mM DTT) containing rel. DNA (150 ng) (TopoGen Inc., Buena Vista, CO, USA) and the tested drugs were added to 0.5 U of *E. coli* gyrase. After 1 h of incubation at 37 °C, the reaction was ended by adding the stop buffer (TopoGEN Inc.; 1% Sarkosyl, 0.025% bromphenolblue, 5% glycerol). Novobiocin (50 µM) was used as a positive control. The reaction mixtures were run on a 1% w/v agarose gels with Tris-acetate/EDTA (TAE) buffer at 4.5 V/cm. Later the gel was placed in 10 mg/L of ethidium bromide solution for 20 min for staining. Fluorescence signals were detected with Image Quant LAS-4000 (GE Healthcare Life Sciences, Buckinghamshire, UK). Fujifilm Image Gauge software (Fujifilm Medical Systems USA, Inc., Lexington, MA USA) was used to detect supercoiled DNA.

Cell cycle analysis

Briefly, 2×10^5 HCT116 cells/well were seeded in 12-well plates and left to recover for 24 h. Cells were treated with indicated concentrations of **3** for further 24 h and then trypsinized, washed with PBS, resuspended in PBS and then dropped into pre-cooled (-20 °C) 70% ethanol. After a fixation of at least 3 h at -20 °C, cells were centrifuged (450 g, 5 min), washed with PBS and taken up in 100 µl of Guava Cell Cycle Reagent (Merck Millipore, USA). After an incubation of 30 min at room temperature, cell fluorescence was measured with a

Guava easyCyte SL 5 flow cytometer (Merck Millipore, USA) in the GuavaSoft 3.1.1 cell cycle program. Analysis was performed with FlowJo software.

Microscopy

Briefly, 2×10^5 HCT116 cells/well were seeded in 12-well plates and left to recover for 24 h. Cells were treated with indicated concentrations of **3** for further 72 h and then imaged using a Zeiss Axiovert microscope. Pictures were adjusted using Fiji software.

Luciferase reporter assay

The firefly luciferase reporter was detected using the ONE-GLO™ Luciferase Assay System (E6120, Promega, Madison, WI, USA). Relative luminescence units (RLU) were measured using the SpectraMax i3x Luminescence Glow Cartridge (Lum 384) (0200-7015POS, Molecular Devices) and normalized to cell count or area determined using the Mini MaxTM 300 Imaging Cytometer (5024062, Molecular Devices). Treatments were performed in triplicate, and fold changes of the different treatments relative to the untreated control sample (NT) were calculated.

Statistics

Statistical analyses and graphs were generated using GraphPad Prism (version 9.03, San Diego, CA, USA). Data are expressed as mean ± standard deviation and significance was accepted at $p \leq 0.05$. One- or two-way ANOVA with post hoc Dunnett's multiple comparison test were used to assess differences between multiple groups, and Student's t-test was performed to compare data between two groups.

Results

Description of novel compounds

The novel okaramine derivative, lemmokaramine (**1**), was obtained after purification following flash and preparative chromatography as yellowish powder. In the mass spectrum it showed a $[M+H]^+$ peak at $m/z = 567.2601$ and a $[M\text{-}H]^-$ peak at $m/z = 565.2463$ corresponding to a molecular formula of $C_{33}H_{34}N_4O_5$. Its ^{1}H NMR spectrum resembled okaramines, such as okaramine A, B or H which contain the azocine substructure, an 8-membered unsaturated N-heterocyclic unit[12]. This structural motif of the okaramines is characterized in the ^{1}H and ^{13}C NMR spectra by the singlet for H-3 at δ_H/δ_C 7.74 / 116.1 ppm and the two doublet signals for H-13 and H-14 at δ_H/δ_C 5.96 / 139.8 ppm and δ_H/δ_C 5.81 / 121.9 ppm with a coupling of $J = 8.2$ Hz. Moreover, compound **1** showed nearly the same substitution pattern on the two annulated five-membered rings as okaramine B: hydroxyl groups on C-2' and C-4' and a methoxyl group at C-3'. But H-11' appeared as broad doublet at δ_H 5.77 ppm coupled to the neighbouring amine proton at δ_H 5.04 ppm. This amine proton showed long range crosspeaks in the HMBC spectrum to C-5' and C-4', whereas H-3' gave correlations to C-1', C-5', C-11' and the methoxyl group supporting the proposed structure. A NOESY crosspeak between H-3' and H-11' indicated the *cis* orientation of these two protons. Finally, one prenyl group could be located at position C-9' proved by the observed HMBC crosspeaks from H-1" to the indole carbons C-8', C-9' and C-10', as well as from from the indol proton H-8' at δ_H 7.05 ppm to the prenyl-CH_2 carbon C-1"at δ_C 29.8 ppm. Therefore, all the NMR spectroscopic and mass spectrometric data are in accordance with the structure for lemmokaramine (**1**) as shown in Fig. 1. ^{1}H and ^{13}C chemical shifts are listed in Table 1.

Besides the above-described lemmokaramine, two other okaramine derivatives, okaramine H (**2**) and okaramine J, as well as the prenylated bisindol diketopiperazines **4**–**6** were isolated from the cultivation media from *Keratinophyton lemmensii*.

The novel tetrahydropyrane, lemmensipyrane (**7**), was obtained after purification following flash and preparative chromatography as white powder. Its molecular formula was determined as $C_{15}H_{22}O_5$ based on its $[M - H]^-$ peak at $m/z = 281.1396$ (calcd 281.1394 for $C_{15}H_{21}O_5$). The ^{1}H NMR spectrum showed signals of five olefinic protons in the range of $\delta_H = 5.5$–7.5 ppm, one methoxy group at $\delta_H = 3.40$ ppm, one singlet methyl at $\delta_H = 1.91$ ppm and one methyl group doublet at $\delta_H = 1.05$ ppm, respectively. By combined analysis of HSQC and ^{1}H NMR spectra three oxymethine (OCH) and one oxymethylene (OCH_2) groups were identified in the range of $\delta_H = 3$–4 ppm, besides one aliphatic CH signal at $\delta_H = 2.23$ ppm. The H, H-COSY spectrum proved that all the olefinic protons formed one spin system (H2 – H6). The doublet methyl group shows a COSY crosspeak to the signal at $\delta_H = 2.23$ ppm (H-11). This proton coupled to the oxymethylene signals (H-12) and also to the oxymethine resonance at $\delta_H = 3.27$ ppm (H-10). The additional crosspeaks H-10/H-9 and H-9/H-8 completed the second spinsystem. C, H long range crosspeaks observed in the HMBC spectrum from both H-12 protons to C-8 and also from H-8 to C-12 proved the presence of the pyrane ring substructure. The connection of these two subunits – the pyrane and the olefinic chain – was established by long range correlations from the singlet methyl protons with C-6, C-7, and C-8, respectively. The methoxyl group was located at C-10 due to the corresponding HMBC crosspeak, whereas long range correlations from H-2 ($\delta_H = 5.87$ ppm) and H-3 ($\delta_H = 7.42$ ppm) to a carbon signal at $\delta_C = 171.2$ ppm indicated a terminal carboxylic acid function. The configuration of the pyrane ring was determined based on analysis of H, H coupling constants in combination with a NOESY spectrum. H-8 and H-9 were both axial due to their characteristic large *axial*/*axial* coupling constant of $J = 9.4$ Hz. H-9 gave a pseudo triplet with a *J* of ca. 9.0 Hz which means that also H-10 had *axial* orientation. H-10 was coupled to H-11 with $J = 5.1$ Hz, typical for *axial*/*equatorial* orientation which was supported also by the small coupling constants from H-11 with both H-12 protons. Finally, all the double bonds were established as *E*-configurated due to their coupling constants of ca. 15 Hz and NOESY crosspeaks between H-6/H-8 and 7-Me/H-5. All the NMR and mass data are in agreement with the lemmensipyrane (**7**) structure as shown in Fig. 2. ^{1}H and ^{13}C chemical shifts are listed in Table 2, relevant HMBC cross-peaks are indicated in Fig. 2.

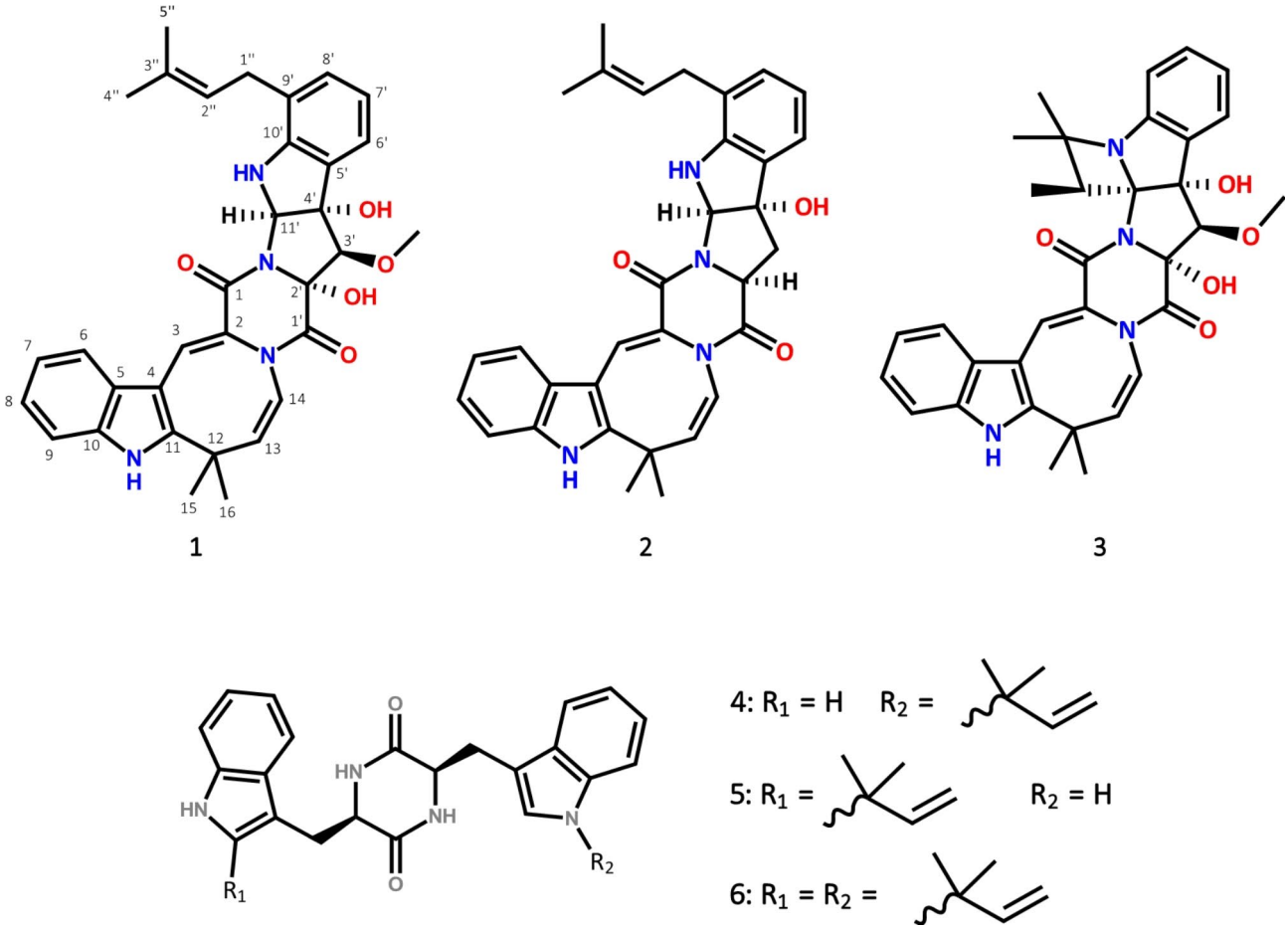

Fig. 1. Structures of lemmokaramine (**1**), okaramine H (**2**)[12], okaramine B (**3**) and tryptophan-based diketopiperazin derivatives **4**–**6** (Shiomoto et al., 1999).

The novel cyclohexyl derivative lemmensihexol (**10**) was obtained after purification following flash and preparative chromatography as white powder. Its molecular formula was determined as $C_{12}H_{20}O_3$ based on its $[M+Na]^+$ peak at $m/z = 235.1304$ (calcd 235.1305 for $C_{12}H_{20}O_3Na$) and its $[M\text{-}H]^-$ peak at $m/z = 211.1342$ (calcd 211.1340 for $C_{12}H_{19}O_3$). The ^{1}H NMR spectrum showed signals of two olefinic protons, one as doublet at $\delta_H = 5.75$ ppm, the other as doublet of doublets at $\delta_H = 6.79$ ppm. This coupling pattern indicated the presence of a CH=CH-CH unit, with their coupling of $J = 15.6$ Hz indicating *trans* configuration of the double bond. In addition, signals of one oxymethine at $\delta_H = 3.83$ ppm and one doublet-type methyl group at $\delta_H = 1.10$ ppm were identified in the ^{1}H NMR spectrum besides resonances of 12 protons at saturated aliphatic carbons in the region of δ_H ca. 1–2 ppm. The ^{13}C chemical shifts of the olefinic carbons with $\delta_C = 120.6$ and 154.8 ppm, respectively, are characteristic for a double bond system with electron-withdrawing group, which was identified as carboxylic acid based on long-range crosspeaks in the HMBC spectrum from both olefinic protons to a carbon signal at $\delta_C = 169.0$ ppm. In addition to the already assigned signals of the unsaturated system (C1-C3), the ^{13}C NMR spectrum showed resonances of one oxymethine carbon ($\delta_C = 66.2$ ppm), two methine carbons ($\delta_C = 47.6 + 38.6$ ppm), one methyl group at $\delta_C = 23.1$ ppm and five methylene signals in the range of $\delta_C = 45 - 20$ ppm. In the H, H COSY spectrum the methyl group (H-12) showed coupling to the oxymethine proton (H-11) which further coupled with protons of a CH_2 group at $\delta_C = 1.42 + 1.26$ ppm (H-10) establishing a CH_3-CH(OH)-CH_2 subunit. Long-range crosspeaks H2/C4, H3/C4,C5,C9 and H11/C9 proved the final structure of compound **10** as a 1,2 disubstituted cyclohexyl derivative as given in Fig. 3. Due to severe overlap of ^{1}H signals the stereochemistry of the asymmetric centers has not been determined. This is part of an ongoing investigation. ^{1}H and ^{13}C chemical shifts are listed in Table 2, relevant HMBC cross-peaks in Fig. 3.

Biological activity

Antimicrobial activity

Antimicrobial activity was evaluated against the Gram-positive bacterium *Staphylococcus aureus* ATCC 6538, the Gram-negative bacteria *Escherichia coli* ATCC 25,922, *Klebsiella pneumoniae* ATCC 10,031 and *Pseudomonas aeruginosa* ATCC 9027, the yeast *Candida albicans* ATCC 10,231, and the filamentous fungus *Aspergillus fumigatus* RL 578. Lemmokaramine (**1**) showed antimicrobial activity against *Staphylococcus aureus* ATCC 6538 and *Candida albicans* ATCC 10,231, with MIC_{50} values between 5 and 7 µg/mL (9–12 µM), and 50–60 µg/

	lemmokaramine (1)		okaramine H (2)	
Position	^{1}H	^{13}C	^{1}H	^{13}C
1	-	163.69	-	163.12
2	-	125.08	-	126.16
3	7.74 (s)	116.10	7.67 (s)	115.29
4	-	105.93	-	105.76
5	-	130.26	-	130.20
6	7.79 (m)	117.90	7.80 (m)	117.92
7	7.22 (m)	121.55	7.22 (m)	121.47
8	7.21 (m)	122.77	7.22 (m)	122.75
9	7.34 (m)	110.98	7.34 (m)	110.97
10	-	133.31	-	133.29
11	-	147.47	-	146.95
12	-	36.24	-	35.88
13	5.96 (d, J = 8.2)	139.82	5.94 (d, J = 8.2)	139.46
14	5.81 (d, J = 8.2)	121.85	5.81 (d, J = 8.2)	122.57
15	1.65 (s)	27.40	1.65 (s)	27.47
16	1.82 (s)	26.78	1.78 (s)	26.38
1’	-	163.80	-	166.49
2’	-	85.45	4.66 (dd, J = 10.5, 6.8)	58.24
3’	4.32 (s)	83.91	2.80 (dd, J = 13.6, 6.8)	40.43
			2.56 (dd, J = 13.6, 10.5)	
4’	-	84.41	-	87.37
5’	-	128.74	-	129.28
6’	7.16 (dd, J = 7.4, 1.0)	120.64	7.21 (m)	120.65
7’	6.83 (ψt, J = 7.4)	120.14	6.81 (ψt, J = 7.4)	120.01
8’	7.05 (dd, J = 7.4, 1.0)	129.95	7.04 (d, J = 7.4)	129.95
9’	-	123.86	-	123.79
10’	-	146.71	-	146.10
11’	5.77 (br.d, J = 3.1)	81.76	5.57 (br.d, J = 3.0)	84.92
1”	3.22 (dd, J = 15.9, 8.0)	29.82	3.22 (dd, J = 15.8, 8.0)	29.75
	3.13 (dd, J = 15.8, 6.6)		3.12 (dd, J = 15.8, 6.3)	
2”	5.27 (m)	120.78	5.22 (m)	120.79
3”	-	134.03	-	134.06
4”	1.77 (d, J = 1.0)	25.71	1.77 (s)	25.74
5”	1.74 (s)	17.89	1.74 (s)	17.90
10-NH	8.52 (br.s)	-	8.46 (br.s)	-
10’-NH	5.04 (br.d, J = 3.1)	-	5.07 (br.d, J = 3.0)	-
OH	-	-	1.66 (br.s)	-
OMe	3.90 (s)	61.20	-	-

Table 1. NMR chemical shifts for lemmokaramine **(1)** and okaramine-H recorded in $CDCl_3$.

mL (92–105 µM), respectively (Table S3). This substance, however, did not show activity against any of the Gram-negative bacteria tested. Lemmensihexol (**10**) showed a weak activity only towards *Staphylococcus aureus* ATCC 6538 at a concentration range of MIC_{50} between 325 and 650 µg/mL (1,5–3 mM), while lemmensipyrane (**7**) showed no antimicrobial activity against any of the tested microbial pathogens even at the highest tested concentration of 650 µg/mL (2,3 mM) (Table S3).

Anticancer activity against colon carcinoma cell models

The substance with the most potent antimicrobial activity, i.e. lemmokaramine (**1**), was tested for further biological activity in mammalian cell culture. To that end, first, cell viability measurements after 72 h were performed with three different colon carcinoma cell models (HT29, HCT116 and SW480) (Fig. 4). These revealed moderate and comparable cytotoxicity in all three cell models with IC_{50} values of 8.3 (HT29), 7.7 (HCT116) and 10.4 µM (SW480). In Caco-2 cells, compound (**1**) had no cytotoxic effect up to a concentration of 20 µM. However, at 40 µM, the substance is significantly toxic when measured immediately after dilution in DMSO (Supplementary I.).

Microscopy of HCT116 cells treated with different concentrations of lemmokaramine (**1**) for 72 h revealed the formation of cytoplasmic vesicles (Fig. 5, arrows), which might indicate either specific forms of cell death such as autophagy[14], paraptosis[15,16] or the formation of lipid droplets that might compartmentalize the compound[17].

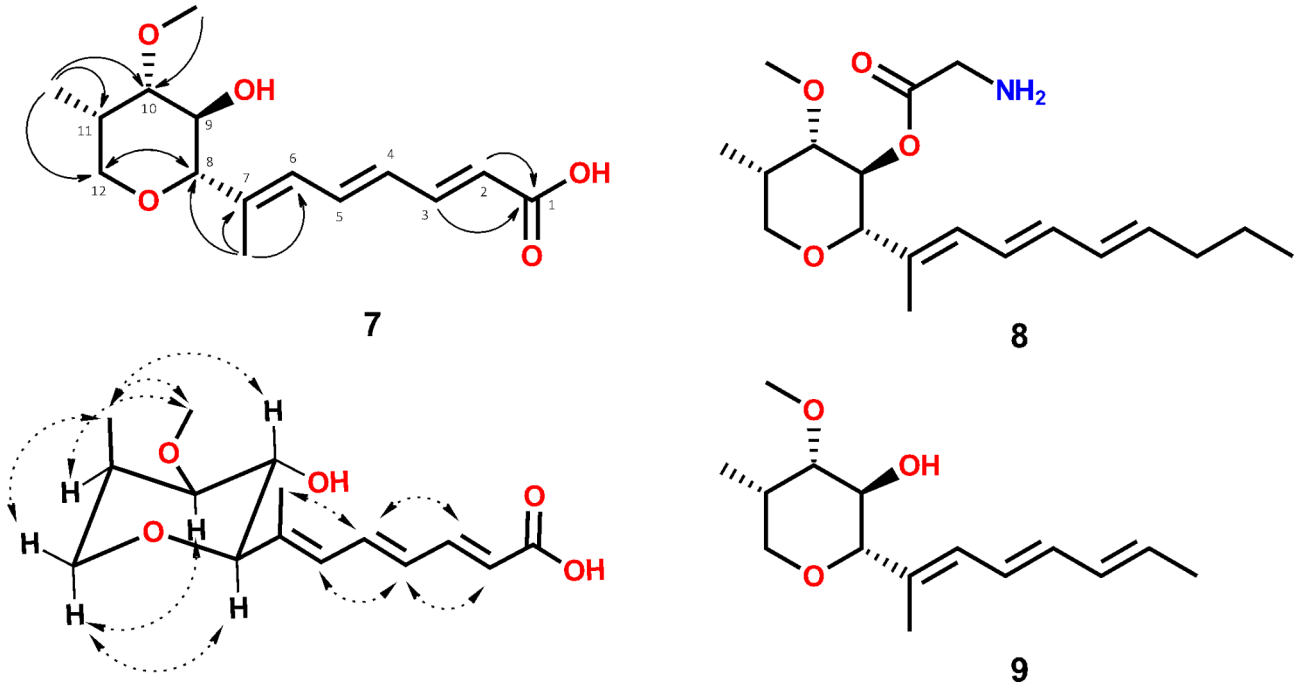

Fig. 2. Structure of lemmensipyrane (**7**) with selected HMBC crosspeaks (top left) and selected NOESY crosspeaks (top right) and related tetrahydropyranes restricticin (**8**[13], and lanomycinol (**9**[14]).

	Lemmensipyrane (7)		Lemmensihexol (10)	
Position	^{1}H	^{13}C	^{1}H	^{13}C
1	-	171.22	-	169.01
2	5.87 (d, *J* = 15.2)	119.57	5.75 (d, *J* = 15.6)	120.65
3	7.42 (dd, *J* = 15.2, 11.4)	146.93	6.79 (dd, *J* = 15.6, 9.5)	154.79
4	6.36 (dd, *J* = 14.8, 11.4)	130.38	1.87 (m)	47.58
5	6.87 (dd, *J* = 14.8, 11.4)	137.07	1.63 + 1.20 (each m)	32.56
6	6.25 (dd, *J* = 11.4, 0.9)	128.25	1.71 + 1.22 (each m)	25.80*
7	-	141.04	1.71 + 1.22 (each m)	25.32*
8	3.54 (d, *J* = 9.3)	95.96	1.82 + 0.96 (each m)	31.90
9	3.63 (t, *J* = 9.1)	67.90	1.24 (m)	38.64
10	3.27 (dd, *J* = 9.0, 5.1)	84.19	1.42 + 1.26 (each m)	44.53
11	2.23 (m)	31.51	3.83 (m)	66.18
12	3.84 (dd, *J* = 11.7, 1.3)	71.11	1.10 (d, *J* = 6.1)	23.09
	3.62 (dd, *J* = 11.7, ??)			
7-Me	1.91 (br.s)	13.07		
11-Me	1.05 (d, *J* = 7.0)	10.76		
OMe	3.40 (s)	55.91		

Table 2. NMR chemical shifts of lemmensipyrane (**7**) and lemmensihexol (**10**) recorded in $CDCl_3$ at 400 MHz.

A potential cellular target for growth inhibition by lemmokaramine (**1**) in both bacteria and human cells might be an inhibition of topoisomerase[18]. Consequently, the potential to inhibit human topoisomerase II α as well as *E. coli* gyrase (both type II topoisomerases) were investigated with decatenation and supercoiling assays, respectively (Fig. 6). Noteworthy, while lemmokaramine (**1**) reduced the decatenation by topoisomerase II α, no detectable reduction in supercoiling activity was observed of bacterial gyrase up to 75 µM of lemmokaramin (**1**).

To test whether the reduction of topoisomerase II α activity also affects the cell cycle of mammalian cells, cell cycle analysis via propidium iodide staining and flow cytometry was performed (Fig. 7). In contrast to an expected cell cycle arrest in S- and/or G2/M phase typical for topoisomerase II poisons[19], treatment of HCT116 cells with lemmokaramine resulted in significant G0/G1 cell cycle arrest at 7.5 and 10 µM. This atypical cell cycle arrest was reminiscent to a substituted 4,5'-bithiozole that was reported to catalytically inhibit topoisomerase II α via competitive ATP inhibition[20].

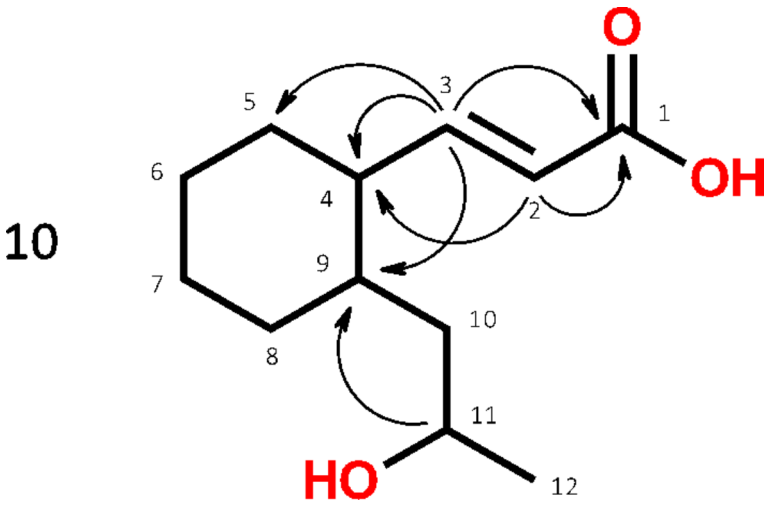

Fig. 3. Structure and selected HMBC crosspeaks of lemmensihexol (**10**).

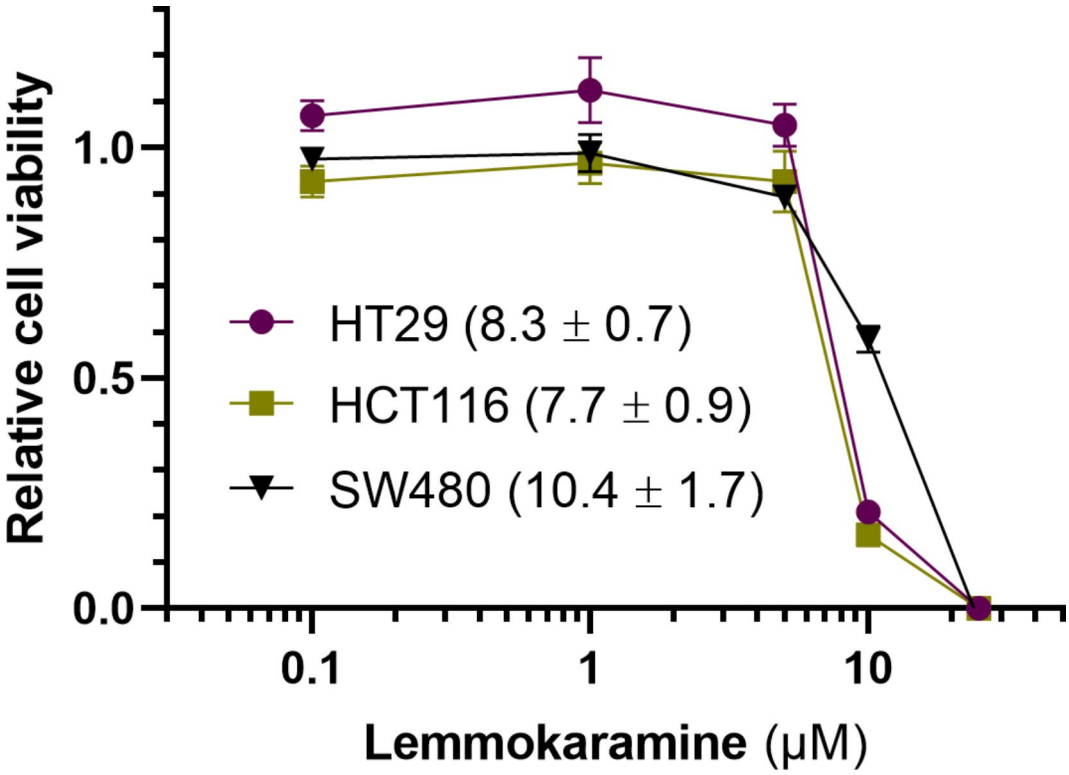

Fig. 4. Cytotoxicity of lemmokaramine (**1**) in three different cancer cell models. Cell viability of HT29, HCT116 and SW480 cells was measured after 72 h treatment with **1** via CellTiter Blue viability assay. Values given are the mean ± standard deviation of triplicates of one representative experiment out of three. IC_{50} values (μM) in the different cell models are given in brackets as mean ± standard deviation of three independent experiments.

Cytotoxicity activity against melanoma cells

We next tested lemmokaramine (**1**) for its anticancerogenic potential against non-metastatic (MCM G1) and metastatic (MCM DLN) melanoma cell lines[21]. To this end, both cell lines were plated in single 96 well plates (20,000 cells/well), treated for 24 h by a $\log_2$ serial dilution and their viability was subsequently assessed by the CellTiter Blue assay. As illustrated in Fig. 8, the melanoma cell lines responded very similar to the substance, but less sensitive compared to the colon cancer cell models with an GI_{50} value of 19.79 μM for MCM G1 and 29.99 μM for MCM DLN. No significant difference could be observed between the two melanoma cell lines and primary melanocytes (data not shown).

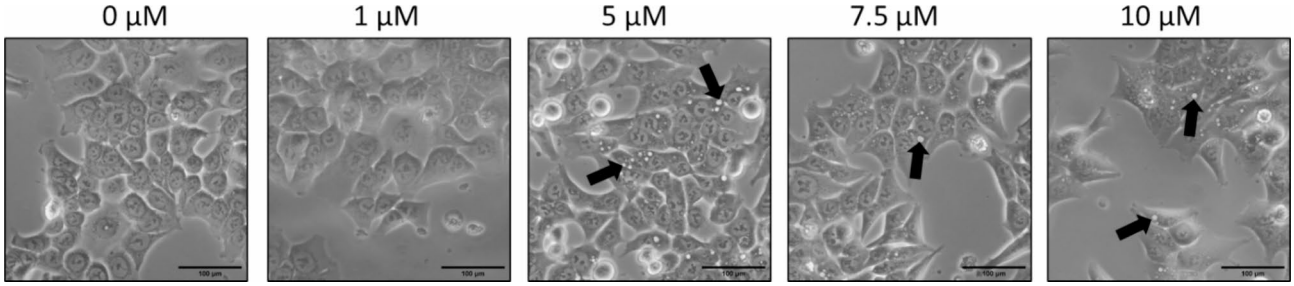

Fig. 5. Morphological changes induced in HCT116 cells after 72 h treatment with increasing concentrations of lemmokaramine (**1**). Arrows indicate the formation of perinuclear vesicles.

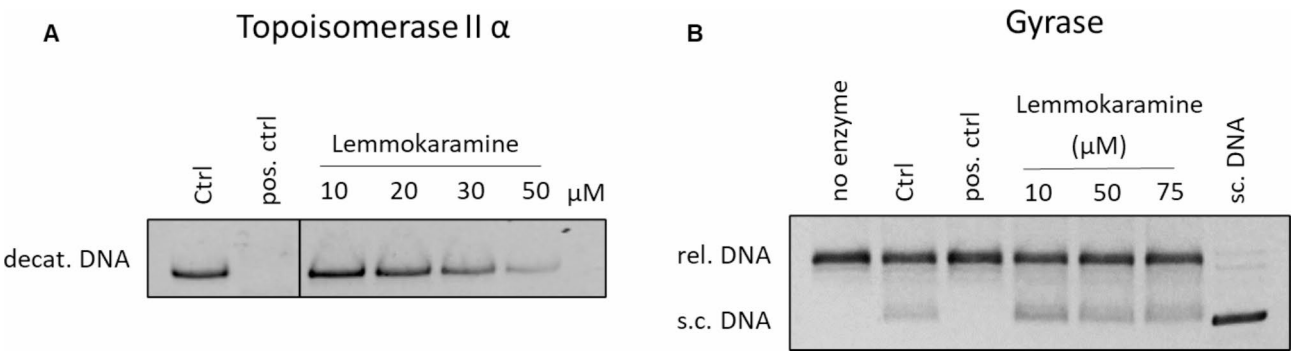

Fig. 6. Cell-free topoisomerase II α and gyrase inhibition by lemmokaramine (**1**). (**A**) Decatenation assay was performed for 1 h with 0.8 U human topoisomerase II α from TopoGEN and 200 ng of kDNA. As positive control (pos. ctrl) 10 µM doxorubicin was used. decat. = decatenated DNA. (**B**) Gyrase inhibition was performed for 1 h with 0.5 U E. coli gyrase from TopoGEN and 150 ng relaxed DNA. As positive control 50 µM novobiocin were used. rel. = relaxed DNA, s.c. = supercoiled DNA.

Effect of lemmokaramine (1) on NRF2 reporter activity in melanoma cells

Oxidants, or reactive oxygen species (ROS), are natural byproducts of energy production in a cell. In low concentrations, they have antimicrobial effects and hence can be used to counteract pathogens, but when present in excess, they can cause protein and DNA damage leading to cell apoptosis[22]. Both pro- and antioxidant compounds could be useful commercial products; prooxidants as additional cancer treatments and antioxidants as dietary supplements[21]. Therefore, we decided to investigate the ability of lemmokaramine to activate an antioxidant NRF-2 pathway and determine its effect on the reporter cell line under native and oxidative stress conditions created by the addition of H_2O_2[11]. For the model, we used a reporter cell line MCM DLN virally transfected with a NRF2-Luc vector (see Methods). The cell line was seeded in a 96-well plate (20,000 cells/well) and allowed to adhere for 24 h. The cells were then treated with the compound at concentrations known from our previous toxicity studies to cause no decrease in cell viability. Treatments were performed with or without 0.25 mM H_2O_2 for 6 h and cell viability was measured by CellTiter Blue viability assay. NRF2 expression in MCM G1 reporter cell line was quantified by luminescence measurement. The luminescence signal normalized to cell viability is presented as relative luminescence units (RLU) in Fig. 9.

As shown in Fig. 9, the reporter activity of Nrf2 in MCM G1 cells is increased 1.4-fold by treatment with 2.5 mM H2O2 for 6 h (NT) and decreased 0.6-fold by the addition of 3 µM lemmokaramine [**1** + H_2O_2], a concentration that does not affect cell viability. Thus, these tests suggest that lemmokaramine has significant antioxidant effects on cultured cells.

Discussion

Okaramines are indole alkaloids first identified in soybean pulp (*okara*) inoculated with *Penicillium simplicissimum*. They were named accordingly okaramine A and B[23], okaramine C[24], D - F[25] and G[26] with very potent broad range insecticidal activity[27]. Okaramines target insect neurons. These fungal compounds were found to act selectively on silkworm larval nerve ion channels and thus induce inward currents[27]. A metabolomic study on soybean rhizospheres suggested that okaramines might be involved in defense of plants against insects[28]. The authors suggested that these substances are similarly responsible for the control of fungal and bacterial diseases[28]. On the other hand[29], isolated several additional okaramine congeners, i.e. okaramines J – M and related compounds from *Penicillium simplicissimum*, and okaramines H and I from *Aspergillus aculeatus*[12], without insecticidal activity against silkworms. We report here production of these compounds by a member of the genus *Keratinophyton* (Onygenales, Ascomycota) which is phylogenetically distant from the genus *Penicillium*

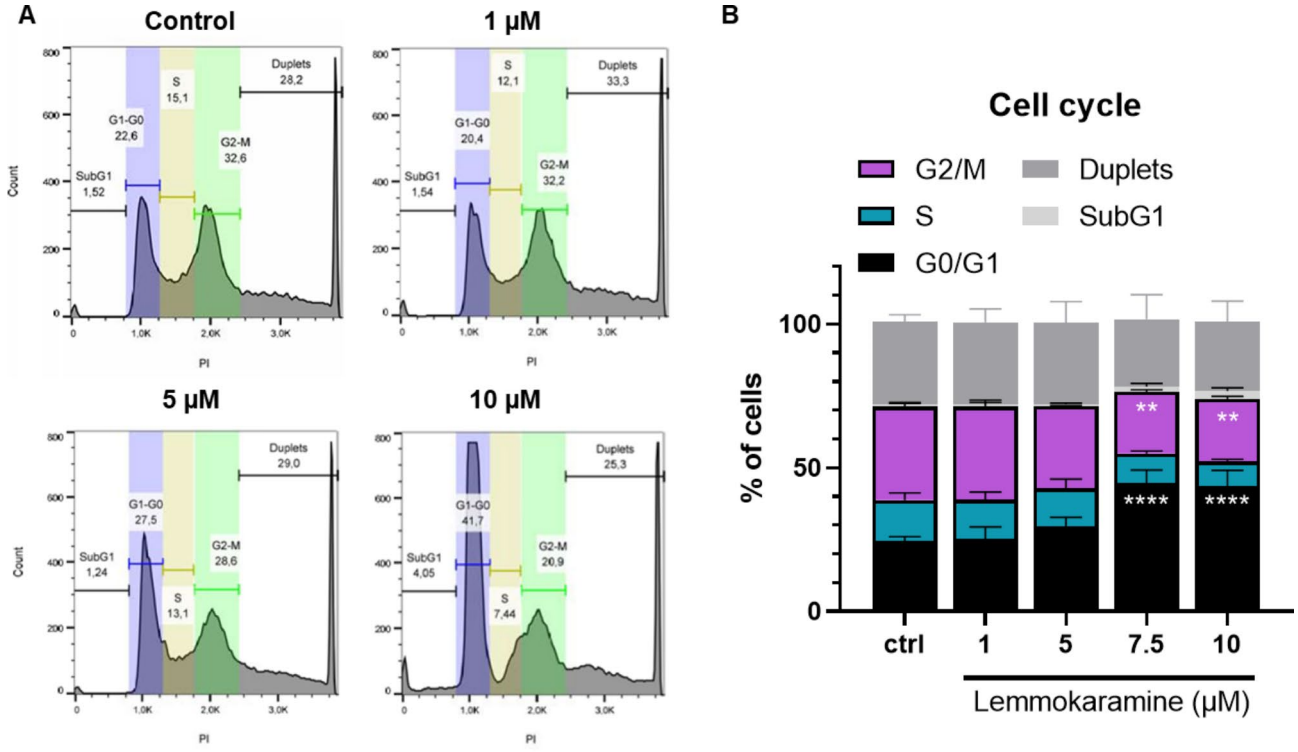

Fig. 7. Cell cycle phase distribution of HCT116 cells after 24 h treatment with lemmokaramine (**1**). Cell cycle changes were measured using propidium iodide staining and flow cytometry. (**A**) Representative fluorescence intensity histograms and cell cycle phase settings analyzed in FlowJo. (**B**) Values given are the mean ± standard deviation of three independent experiments. Significance to control was calculated using two-way Anova and Dunnett's multiple comparisons test (* $p \leq 0.05$; ** $p \leq 0.01$; *** $p \leq 0.001$; **** $p \leq 0.0001$).

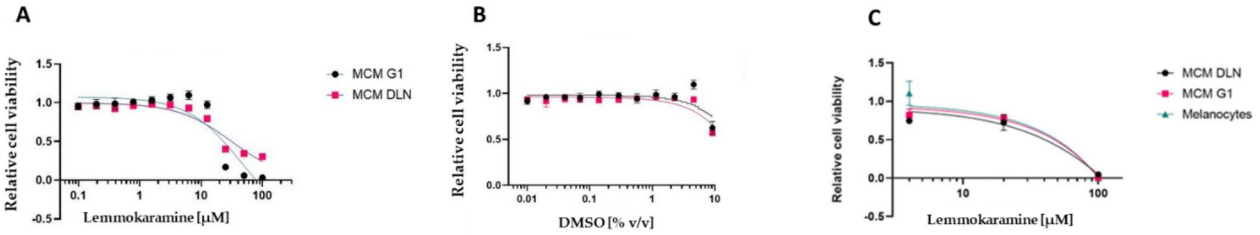

Fig. 8. Effect of lemmokaramine (1) on the viability of MCM G1 and MCM DLN cells. The monolayers (seeded at 20,000 cells/well) were treated with (**A**) lemmokaramine or (**B**) the same volume of DMSO for 24 h after cell seeding with a serial $\log_2$ dilution (initial concentration of lemmokaramine was 100 µM and 4.58%v/v DMSO)). Cell viability was determined 24 h after treatment with CellTiter Blue viability assay. The experiment was performed in triplicates and normalised to non-treated cell (NT). The graph shows the mean of the 3 observations and their corresponding SD. Due to the x-axis being logarithmic it is not showing the NT value at point $x = 0,\ y = 1$.

(Eurotiales, Ascomycota)[30]. Three congeners of okaramines, namely cyclo (6a′-(α,α-dimethylallyl)-$_L$-Trp-$_L$-Trp) (**5**), cyclo (N^8-(α,α-dimethylallyl)-$_L$-Trp-$_L$-Trp) (**4**) and especially a novel compound lemmokaramine (**1**), were found to be active against Gram-positive bacterium *Staphylococcus aureus* and yeast fungus *Candida albicans*.

With regard to mammalian cells and anticancer activity, lemmokaramine (**1**) induced several interesting biological effects. The compound did not only decrease viability in all tested cancer cell models (except Caco-2 cells) above concentrations of 12.5 µM, but also induced cell cycle arrest in colon carcinoma HCT116 cells significantly at concentrations above 7.5 µM. Additionally, microscopy of HCT116 cells treated with lemmokaramine (**1**) revealed the formation of cytoplasmic vesicles, which might indicate either forms of cell death such as autophagy or paraptosis[14,15], or the formation of lipid droplets that might compartmentalize the compound[17]. A potential reason for the growth inhibition by lemmokaramine (**1**) in both bacteria and human cells might be an inhibition of the enzyme topoisomerase, which is structurally similar in both organisms[18]. Our tests revealed that lemmokaramine (**1**) has some activity as it reduced the decatenation by topoisomerase

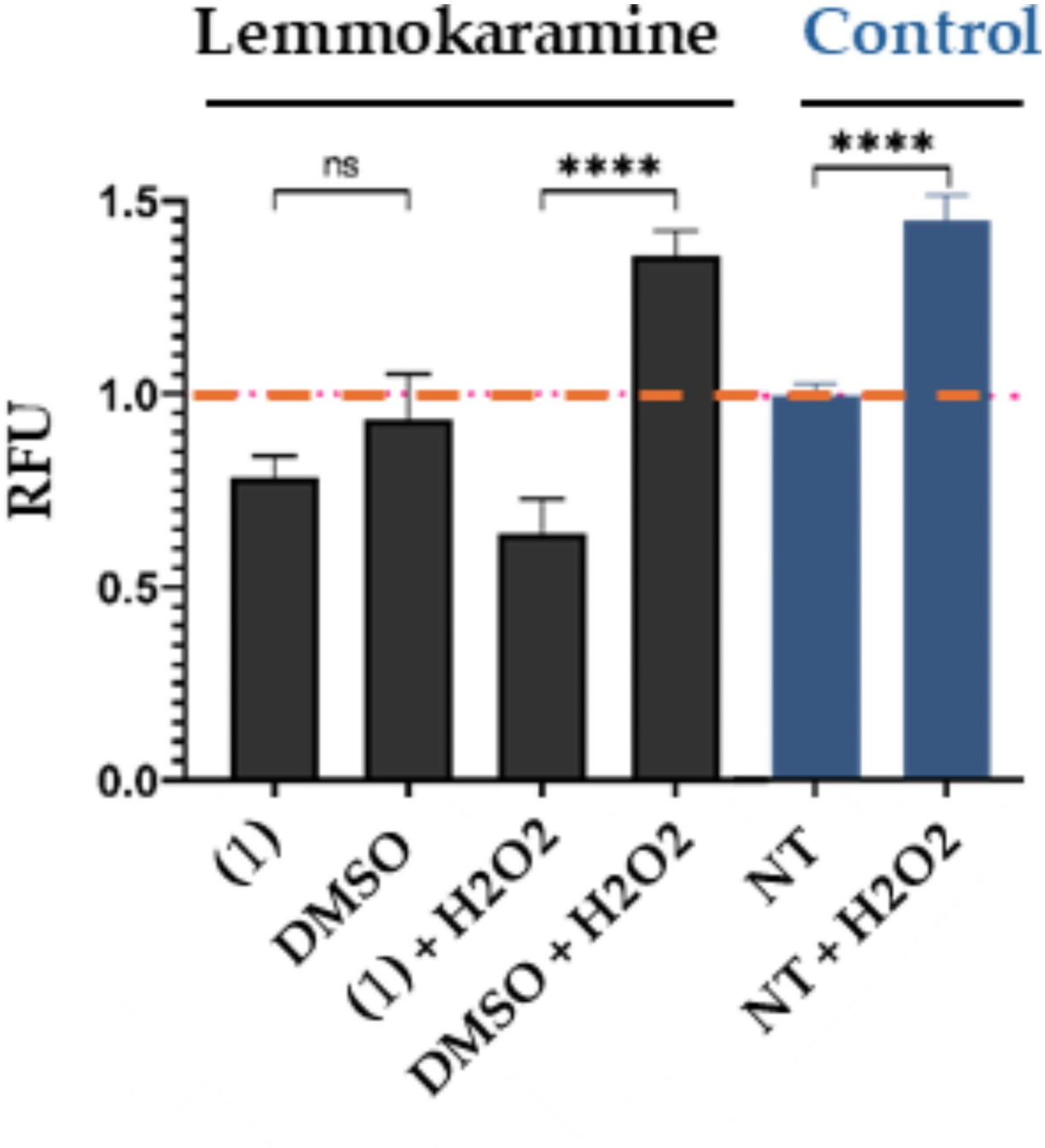

Fig. 9. The effect of lemmokaramine (**1**) on MCM DLN NRF-2 Luc cells. MCM DLN NRF2 Luc cells (seeded at 20,000 cells/well) were treated 24 h after seeding with 3 µM lemmokaramine (non-toxic concentration) or DMSO only and 0.25 mM H_2O_2. After 6 h, viability and luminescence were determined and normalized to non-treated (NT) cells, resulting in relative luminescence units (RLU). The graphs show the mean of the 3 observations and the corresponding SD. For controls, the significance of H_2O_2 treatment on RLU is shown. Significance is shown as *p*-values; **** = $p < 0.0001$ and ns = not significant.

II α, although no detectable reduction in supercoiling activity by bacterial gyrase was observed up to 75 µM of lemmokaramine (**1**). In addition to these effects, we could determine that higher concentrations (> 12.5 µM) of lemmokaramine (**1**) reduce melanoma growth in both MCM 1G (non-metastatic melanoma) and MCM DLN (metastatic melanoma) cell lines, whereas low concentrations (6.3 µM–1.6 µM) indicate the opposite effect. Similar effects were observed in the colon carcinoma cell line HT29, although not with SW480 and HCT116 cells. Beside the inhibition of the enzyme topoisomerase II α and cell cycle arrest, the antitumorigenic effect could be due to pro-oxidant properties of lemmokaramine (**1**). Naturally occurring small molecules such as polyphenols, carotenoids, betaines etc. can act as pro- or antioxidants. The pro-oxidant activities are supported by their capacity to generate phenoxyl radicals or produce reactive oxygen species (ROS) in the presence of transition metals. In the presence of oxygen, phenoxyl radicals are capable of producing O_2-*, H_2O_2, quinones, and semiquinones. There is an increasing body of evidence that highlights the dual nature of ROS in cancer cells[31,32]. At low to moderate levels, ROS may be regarded as signaling molecules, orchestrating processes such as cancer cell growth, migration, invasion, and drug resistance[33,34]. However, when ROS levels are increased, they become harmful to cancer cells, ultimately leading to their destruction[21,35,36]. ROS act as both promoters and executioners of cancer cell functions. Consequently, using lemmokaramine (**1**) for generating ROS, inducing cell cycle arrest via topoisomerase II α inhibition might be a useful tactic in the fight against cancer.

The process of detoxification is orchestrated by a network of redox-modulating enzymes that operate within cells to diminish the levels of ROS and toxic metabolites. The transcription factor Nrf2 has been identified as a pivotal regulator of the cellular antioxidant defense mechanisms. A number of ROS-detoxifying enzymes, including SOD, catalase, GPX1, and thioredoxin, have been recognized as downstream effectors of the Nrf2/Keap1 pathway[37]. A Nrf-2 reporter cell line[21] was employed to demonstrate that lemmokaramine (**1**) can markedly reduce H_2O_2-induced NRF2 activity at low concentrations (3 µM), indicating that lemmokaramine has notable antioxidant effects on cultured cells. Excessive production of ROS can lead to oxidative damage to biomolecules, contributing to aging and several diseases, including cancer, cardiovascular and neurodegenerative disorders[38]. Therefore, lemmokaramine (1) may be a valuable supplement to help prevent or combat these conditions.

We isolated and characterized the compound lemmensipyrane (**7**). Structurally similar polyketide and tetrahydropyran compounds such as lanomycinol, lanomycin and their derivatives, e.g. restricticin, are exhibiting antifungal and antibacterial[13,39–44], anti-neuroinflammatory[45], and anti-tumor[46] properties. For Anti-neuroinflammatory effects of restricticin B by suppressing the production of pro-inflammatory mediators in activated cells have been reported[45]. We find a weak activity against the Gram-positive bacterium *Staphylococcus aureus*, which has not been investigated further. However, we note that the structural similarity to other physiologically active tetrahydropyrans warrants further exploration. Fungi able to produce these compounds were reported previously to belong to the genus *Westerdykella* (*W. dispersa*)[13], *Penicillium* sp. NR6564 and *Aspergillus* (*A.sclerotiorum*[39], *Pycnidiophora dispersa*[47], Penicillium (*P. janthinellum*[45], *P. restrictum*[42]), and *Chaetomium* sp[46]. Therefore, the genus *Keratinophyton* represents a potentially new source for bioactive compounds.

There are only a few reports about compounds structurally similar to lemmensihexol (**10**), such as cyclohexane derivatives[48] and the bradykinin antagonist pseudopeptide derivatives of aminoalkenoic acids[49]. In this latter case, there is no published information about biological activities of these similar compounds. The biological role metabolite for the fungus is currently unclear. In our tests, lemmensihexol (**10**) showed some weak activity against all microbial species tested.

Conclusions

The filamentous fungus *Keratinophyton lemmensii* BiMM-F76 was cultivated on solid medium on about 160 plates (4 L) containing modified yeast extract sucrose medium for seven weeks at 25 °C in the dark. The crude ethyl acetate extract (4 g) was purified by reverse-phase silica gel flash chromatography, and its fractions were tested by disc diffusion methods against six microbial pathogens, including Gram-positive (1sp.), Gram-negative (3 spp.) and fungi (2 spp.) and followed by preparative HPLC. Consequently, an active fraction F4 contained two known okaramine congeners, cyclo (6a´-(α,α-dimethylallyl)-$_L$-Trp-$_L$-Trp)(**5**) and cyclo (N^8-(α,α-dimethylallyl)-$_L$-Trp-$_L$-Trp)(**4**) with a total yield of 4.5 mg and 1.5 mg, respectively. These two substances were active against *Staphylococcus aureus* ATCC 6538. Additionally, two novel compounds, namely a novel tetrahydropyrane, named lemmensipyrane (**7**) and novel cyclohexyl, named lemmensihexol (**10**) were, isolated and identified with total yields 11.3 mg and 17.6 mg, respectively. These two novel substances did not show antimicrobial activity against any of the microbial pathogens tested in this study.

The second active fraction (F5) contained a new okaramine congener, named lemmokaramine (**1**) with yield of 23 mg, showing antimicrobial activity against *Staphylococcus aureus* ATCC 6538 and *Candida albicans* ATCC 10,231, with MIC_{50} 5–7 µg/mL (9–12 µM), and 50–60 µg/mL (92–105 µM), respectively. The new okaramine was also found to be cytotoxic against different mammalian cell lines (Caco-2, MCM G1, and MCM DLN). Furthermore, by measuring Nrf2 reporter activity, we found a significant antioxidant effect of lemmokaramine following H_2O_2 treatment. All chemical structures were elucidated by NMR and LC-MS, and they will be further investigated for their potential as insecticidal, antiparasitic or anti-tumor agents.

Data availability

The data presented in this study are available in supplementary material and/or from the author. The datasets generated for *Keratinophyton lemmensii* are available in the NCBI repository, https://www.ncbi.nlm.nih.gov/ under MN633082 (ITS) and MT874998 (LSU).

Received: 6 August 2024; Accepted: 7 October 2024

Published online: 25 October 2024

References

1. Labuda, R. et al. Molecular systematics of Keratinophyton: The inclusion of species formerly referred to Chrysosporium and description of four new species. *Ima Fungus*. **12** https://doi.org/10.1186/s43008-021-00070-2 (2021).
2. Kandemir, H. et al. Phylogenetic and ecological reevaluation of the order Onygenales. *Fungal Divers.* **115**, 1–72. https://doi.org/10.1007/s13225-022-00506-z (2022).
3. Li, X. et al. Keratinophyton chongqingense sp. nov. and keratinophyton sichuanense sp. nov., from soil in China. *Int. J. Syst. Evol. Microbiol.* (2022).
4. Macheleidt, J. et al. Regulation and role of fungal secondary metabolites. *Annu. Rev. Genet.* **50**, 371–392. https://doi.org/10.1146/annurev-genet-120215-035203 (2016).
5. Corbu, V. M., Gheorghe-Barbu, I., Dumbrava, A. S., Vrancianu, C. O. & Sesan, T. E. Current insights in fungal importance-a comprehensive review. *Microorganisms*. **11**, 1384. https://doi.org/10.3390/microorganisms11061384 (2023).
6. Aldholmi, M., Marchand, P., Ourliac-Garnier, I., Le Pape, P. & Ganesan, A. A decade of antifungal leads from natural products: 2010–2019. *Pharmaceuticals (Basel)*. **12**, 182. https://doi.org/10.3390/ph12040182 (2019).
7. Lin, Z., Kakule, T. B., Reilly, C. A., Beyhan, S. & Schmidt, E. W. Secondary metabolites of Onygenales fungi exemplified by aioliomyces pyridodomos. *J. Nat. Prod.* **82**, 1616–1626. https://doi.org/10.1021/acs.jnatprod.9b00121 (2019).
8. Kushwaha, R. K. & Guarro, J. *Biology of Dermatophytes and Other Keratinophilic fungi* (Revista Iberoamericana de Micologia, 2000).
9. Samson, R. A., Houbraken, J., Thrane, U., Frisvad, J. C. & Andersen, B. *In CBS Laboratory Manual Series* 310 (pp (CBS-KNAW Fungal Biodiversity Centre Utrecht, 2010).
10. Hensens, O. D. et al. Structure elucidation of restricticin, a novel antifungal agent from penicillium restrictum. *Tetrahedron*. **47**, 3915–3924. https://doi.org/10.1016/S0040-4020(01)86432-2 (1991).
11. Muller, U. et al. In vitro and in vivo inhibition of intestinal glucose transport by guava (*Psidium guajava*) extracts. *Mol. Nutr. Food Res.* **62**, e1701012. https://doi.org/10.1002/mnfr.201701012 (2018).
12. Hayashi, H., Furutsuka, K., Shiono, Y. & Okaramines, H. I, new okaramine congeners, from *Aspergillus Aculeatus*. *J. Nat. Prod.* **62**, 315–317. https://doi.org/10.1021/np9802623 (1999).
13. Xu Dan, P. X. J. & Ting, Z. New alkenylated tetrahydropyran derivatives from the marine sediment-derived fungus *Westerdykella dispersa* and their bioactivities. *Fitoterapia*. **122**, 45–51. https://doi.org/10.1016/j.fitote.2017.08.010 (2017).
14. Wang, C. W. & Klionsky, D. J. The molecular mechanism of autophagy. *Mol. Med.* **9**, 65–76 (2003).
15. Park, W. et al. Diversity and complexity of cell death: A historical review. *Exp. Mol. Med.* **55**, 1573–1594. https://doi.org/10.1038/s12276-023-01078-x (2023).
16. Hager, S. et al. The thiosemicarbazone me(2)NNMe(2) induces paraptosis by disrupting the ER thiol redox homeostasis based on protein disulfide isomerase inhibition. *Cell. Death Dis.* **9**, 1052. https://doi.org/10.1038/s41419-018-1102-z (2018).
17. Antunes, P., Cruz, A., Barbosa, J., Bonifacio, V. D. B. & Pinto, S. N. Lipid droplets in cancer: From composition and role to imaging and therapeutics. *Molecules*. **27**, 991. https://doi.org/10.3390/molecules27030991 (2022).
18. Dalvie, E. D. & Osheroff, N. in *Encyclopedia of Biological Chemistry III* (ed Joseph Jez) 479–486 Elsevier, (2021).
19. Soliman, T. N., Keifenheim, D., Parker, P. J. & Clarke, D. J. Cell cycle responses to Topoisomerase II inhibition: Molecular mechanisms and clinical implications. *J Cell Biol* 222. (2023). https://doi.org/10.1083/jcb.202209125
20. Bergant Loboda, K. et al. Substituted 4,5'-Bithiazoles as catalytic inhibitors of human DNA topoisomerase II alpha. *J. Chem. Inf. Model.* **60**, 3662–3678. https://doi.org/10.1021/acs.jcim.0c00202 (2020).
21. Hundsberger, H. et al. Concentration-dependent pro- and antitumor activities of quercetin in human melanoma spheroids: Comparative analysis of 2D and 3D cell culture models. *Molecules*. **26** https://doi.org/10.3390/molecules26030717 (2021).
22. Pizzino, G. et al. Oxidative stress: Harms and benefits for Human Health. *Oxid. Med. Cell. Longev.* **2017** (8416763). https://doi.org/10.1155/2017/8416763 (2017).
23. Hayashi, H., Takiuchi, K., Murao, S. & Arai, M. Structure and insecticidal activity of new indole alkaloids, okaramines A and B, from *Penicillium simplicissimum* AK-40. *Agric. Biol. Chem.* **53**, 461–469. https://doi.org/10.1080/00021369.1989.10869287 (2014).
24. Hayashi, H., Fujiwara, T., Murao, S., Arai, M. & Okaramine -C, a new insecticidal indole alkaloid from *Penicillium Simplicissimum*. *Agric. Biol. Chem.* **55**, 3143–3145. https://doi.org/10.1080/00021369.1991.10857916 (1991).
25. Hayashi, H., Asabu, Y., Murao, S. & Arai, M. New okaramine ccongeners, okarimines D, E, and F, from Penicillium Simplicissimum ATCC 90288. *Bioscience Biotechnol. Biochem.* **59**, 246–250. https://doi.org/10.1271/bbb.59.246 (1995).
26. Hayashi, H., Sakaguchi, A. & Okaramine, G. A new okaramine congener from *Penicillium Simplicissimum* ATCC 900288. *Bioscience Biotechnol. Biochem.* **62**, 804–806. https://doi.org/10.1271/bbb.62.804 (1998).
27. Matsuda, K. Okaramines and other plant fungal products as new insecticide leads. *Curr. Opin. Insect Sci.* **30**, 67–72. https://doi.org/10.1016/j.cois.2018.09.010 (2018).
28. Sakurai, N. et al. Metabolome analysis identified okaramines in the soybean rhizosphere as a legacy of hairy vetch. *Front. Genet.* **11**. (2020).
29. Shiono, Y., Akiyama, K. & Hayashi, H. New okaramine congeners, okamines J, K, L, M and related compounds, from ATCC 90288. *Bioscience Biotechnol. Biochem.* **63**, 1910–1920. https://doi.org/10.1271/bbb.63.1910 (1999).
30. Houbraken, J. et al. Classification of aspergillus, penicillium, talaromyces and related genera (eurotiales): An overview of families, genera, subgenera, sections, series and species. *Stud. Mycol.* **95**, 5–169. https://doi.org/10.1016/j.simyco.2020.05.002 (2020).
31. Snezhkina, A. V. et al. ROS generation and antioxidantd defense systems in normal and malignant cells. *Oxid. Med. Cell. Longev.* **2019** (6175804). https://doi.org/10.1155/2019/6175804 (2019).
32. Yang, H. et al. The role of cellular reactive oxygen species in cancer chemotherapy. *J. Exp. Clin. Cancer Res.* **37**, 266. https://doi.org/10.1186/s13046-018-0909-x (2018).
33. Wiseman, H. & Halliwell, B. Damage to DNA by reactive oxygen and nitrogen species: role in inflammatory disease and progression to cancer. *Biochem. J.* **313** (Pt 1), 17–29. https://doi.org/10.1042/bj3130017 (1996).
34. Okon, I. S. & Zou, M. H. Mitochondrial ROS and cancer drug resistance: Implications for therapy. *Pharmacol. Res.* **100**, 170–174. https://doi.org/10.1016/j.phrs.2015.06.013 (2015).
35. Leon-Gonzalez, A. J., Auger, C. & Schini-Kerth, V. B. Pro-oxidant activity of polyphenols and its implication on cancer chemoprevention and chemotherapy. *Biochem. Pharmacol.* **98**, 371–380. https://doi.org/10.1016/j.bcp.2015.07.017 (2015).
36. Gorrini, C., Harris, I. S. & Mak, T. W. Modulation of oxidative stress as an anticancer strategy. *Nat. Rev. Drug Discov.* **12**, 931–947. https://doi.org/10.1038/nrd4002 (2013).
37. DeNicola, G. M. et al. Oncogene-induced Nrf2 transcription promotes ROS detoxification and tumorigenesis. *Nature*. **475**, 106–109. https://doi.org/10.1038/nature10189 (2011).
38. Yang, S. & Lian, G. ROS and diseases: Role in metabolism and energy supply. *Mol. Cell. Biochem.* **467**, 1–12. https://doi.org/10.1007/s11010-019-03667-9 (2020).
39. Matsukuma, S. et al. A new series of natural antifungals that inhibit P450 lanosterol C-14 demethylase. I. Taxonomy, fermentation, isolation and structural elucidation. *J. Antibiot. (Tokyo)*. **45**, 151–159. https://doi.org/10.7164/antibiotics.45.151 (1992).
40. Jendrzejewski, S. & Ermann, P. Total synthesis of restricticin. *Tetrahedron Lett.* **34**, 615–618. https://doi.org/10.1016/S0040-4039(00)61633-7 (1993).

41. Paterson, I. & Nowak, T. Anti aldol reactions of α-alkoxymethyl ketones: application to the total synthesis of (+)-restricticin. *Tetrahedron Lett.* **37**, 8243–8246. https://doi.org/10.1016/0040-4039(96)01879-5 (1996).
42. Schwartz, R. E. et al. Restricticin, a novel glycine-containing antifungal agent. *J. Antibiot. (Tokyo).* **44**, 463–471. https://doi.org/10.7164/antibiotics.44.463 (1991).
43. O'Sullivan, J. et al. Lanomycin and glucolanomycin, antifungal agents produced by Pycnidiophora dispersa. I. Discovery, isolation and biological activity. *J. Antibiot. (Tokyo).* **45**, 306–312. https://doi.org/10.7164/antibiotics.45.306 (1992).
44. Liu, N. et al. Targeted genome mining reveals the biosynthetic gene clusters of naturalpProduct CYP51 inhibitors. *J. Am. Chem. Soc.* **143**, 6043–6047. https://doi.org/10.1021/jacs.1c01516 (2021).
45. Choi, B. K. et al. Anti-neuroinflammatory agent, restricticin B, from the marine-derived fungus *penicillium janthinellum* and its inhibitory activity on the NO production in BV-2 microglia cells. *Mar. Drugs*. **18**, 465. https://doi.org/10.3390/md18090465 (2020).
46. Aly, A. H. et al. A new tetrahydrofuran derivative from the endophytic fungus Chaetomium sp. isolated from *Otanthus Maritimus*. *Z. Naturforsch C J. Biosci.* **64**, 350–354. https://doi.org/10.1515/znc-2009-5-608 (2009).
47. Phillipson, D. W., O'Sullivan, J., Johnson, J. H., Bolgar, M. S. & Kahle, A. D. Lanomycin and glucolanomycin, antifungal agents produced by Pycnidiophora dispersa. II. Structure elucidation. *J. Antibiot. (Tokyo).* **45**, 313–319. https://doi.org/10.7164/antibiotics.45.313 (1992).
48. Fujita Atsuko, M. S., Kazutoshi, M., Hiroyuki, T. & Fusayuki, T. Nakagawa Etsuo. Cyclohexane derivatives, liquid-crystal composition, and liquid-crystal display element. (1998).
49. Kyle, D. J. Bradykinin antagonist pseudopeptide derivatives of aminoalkenoic acids. (1996).

Acknowledgements

We thank Sandrina Wimmer for excellent operative support and acknowledge Open Access Funding by the University of Veterinary Medicine Vienna. We also thank Daniel Piller for assisting with some of the cytotoxicity experiments. The laboratory infrastructure was kindly provided by the BOKU Core Facility Bioactive Molecules: Screening and Analysis (CF-BMoSA).

Author contributions

Conceptualization, R.L. and J.S.; Data curation, M.D. and C.S.; Formal analysis, R.L., M.B., H.G., M.D., S.H., M.O., N.O., and C.W.; Funding acquisition, M.W. and J.S.; Investigation, R.L.; Methodology, R.L., D.M., C.W., and S.H.; Resources, J.S.; Supervision, D.M., C.W., M.W., C.S. and T.R.; Writing—original draft, R.L., M.B., J.S. and C.S.; Writing—review & editing. All authors have read and agreed to the published version of the manuscript.

Funding

The research platform Bioactive Microbial Metabolites (BiMM) is supported by grants K3-G-2/026-2013 and COMBIS/LS16005 funded by the Gesellschaft für Forschungsförderung Niederösterreich m.b.H.

Declarations

Competing interests

The authors declare no competing interests.

Additional information

Supplementary Information The online version contains supplementary material available at https://doi.org/10.1038/s41598-024-75510-1.

Correspondence and requests for materials should be addressed to R.L. or J.S.